

# Modelado mesoscópico de un crudo pesado para predecir tensión Interfacial

## Heavy crude oil mesoscopic modeling to predict interfacial tension

**Silva, Carolina del Valle**

Universidad Central de Venezuela, Ciudad Universitaria, Caracas, Venezuela.  
Intevep, S.A, El Tambor, Los Teques, Edo. Miranda,  
Caracas, 1020-A, Venezuela.  
carolinasil@gmail.com

DOI: <https://doi.org/10.53766/CEI/2022.43.03.07>

### Resumen

*Los crudos pesados representan un porcentaje significativo de las reservas de petróleo disponibles en el mundo, parte de las cuales están localizadas en Venezuela. Estos crudos tienen un alto nivel de complejidad debido a su alto contenido de asfaltenos, presencia de metales pesados y heteroátomo, que los convierten en fluidos altamente viscosos; propiedades que dificultan su estudio a nivel teórico y experimental. A pesar del poder computacional actual, aun no es factible estudiar estos sistemas, expresados en sus constituyentes principales, a un nivel atomístico. Considerando este hecho, se realizó la representación y estudio a escala mesoscópica, de un crudo pesado venezolano, con base en datos teóricos y experimentales, modelado aplicando Dinámica de Partículas Disipativas (DPD) y la técnica de grano grueso. Las partículas DPD se corresponden con las fracciones principales del crudo pesado, para lo cual se realizó un super-graneado de cada fracción, lo que implica un nuevo enfoque en la representación de un sistema de crudo pesado. La validación de los modelos se realizó estudiando su comportamiento en la interface, evaluando la evolución de la tensión interfacial, perfiles de densidad e imágenes obtenidas de las dinámicas realizadas, de acuerdo a las variaciones de las concentraciones del crudo, sus fracciones y solventes utilizados. Los resultados obtenidos, reprodujeron exitosamente el comportamiento y las tendencias reportadas, bajo condiciones similares y apoyan la validez y ventaja del enfoque del presente estudio, como una alternativa para el análisis, predicción y comprensión del comportamiento en la interface de este tipo de sistemas.*

**Palabras clave:** Modelo de crudo pesado, Grano-Grueso, Modelado Mesoscopico, Dinámica de Partículas Disipativas, Tensión Interfacial.

### Abstract

*Heavy crude oils represent a significant percentage of oil reserve available in the world, part of which are located in Venezuela. Nevertheless, they have a high level of complexity due to the asphaltenes, heavy metals, and heteroatoms presence which converts these crudes into highly viscous fluids. These properties make difficult its theoretical and experimental study. Despite the computational power today, it is not feasible to represent and study these systems, expressing their principal constituents at the atomistic level. Considering this fact, the study of a heavy crude from Venezuela was carried out, at a mesoscopic scale, based on theoretical and experimental data, modeled by applying Dissipative Particle Dynamics (DPD), and the coarse-graining technique. DPD beads correspond to the heavy crude oil main fractions, for which a super-grain of each fraction was made, implying a new approach in a heavy crude oil system representation. The models' validation was done by studying the behavior of the systems at the interface, evaluating the interfacial tension evolution, density profiles, and images obtained from the dynamic performed, according to the variations of the concentrations of the heavy crude oil, their fractions, and solvents used. The results successfully reproduced the behavior and trends reported for these systems, under similar conditions, and support the validity and advantage of the approach of the present study, as an alternative for the analysis, prediction and understanding of the behavior in the interface of this type of systems.*

**Keywords:** Heavy crude model, Coarse-Graining, Dissipative Particle Dynamics, mesoscopic modeling, Interfacial Tension.

## 1 Introducción

Heavy crude currently represents a significant percentage of the oil reserves available in the world. Among the main features of this energy resource is the presence of asphaltenes, high organometallic compounds content, and heteroatoms, which make them extremely viscous fluids.

These properties make it difficult both for its recovery, as its study and understanding. From the theoretical point of view, despite the technological developments that have significantly increased computing power, today it is not feasible to represent and study in detail these systems at the atomistic level. Fact that has driven the design of new models and computational techniques more efficient, focused on exploring this type of system at a mesoscopic scale.

Dissipative particles dynamics (DPD) is among these techniques, which has been successfully applied in studying a wide variety of systems between them, petroleum fluids systems (Em Karniadakis et al., 2014; Guo et al., 2013; Xu et al., 2014; Li et al., 2013; Xu et al., 2019; Fang et al., 2017; Rojas-Solorzano et al., 2017; Xu et al., 2015; Modarress et al., 2016). This description level allows carrying out numerical studies focused on the understanding and predicting parameters of interest, such as the interfacial tension estimation and aggregation mechanisms associated with variations in concentrations of crude-solvent, among others.

On this matter, a mesoscopic model of heavy crude oil from Venezuela is proposed. Accordingly, Section 1 presents a summary of the main characteristics of petroleum fluids. Section 2 presents the mesoscopic technique methodology used. In Section 3, the mesoscopic model proposed for heavy crude oil is detailed. Section 4 shows the results obtained, and conclusions are presented in Section 5.

### 1.1 Main properties of crude oil

Petroleum is a multiphase fluid, consisting mainly of hydrocarbons, organic and inorganic compounds, which present a wide range of sizes, shapes, structures, and distribution of molecular weights. In nature, there are seven well-known types of petroleum fluids which, according to their fluidity, are classified as natural gas, condensed gas, light crudes, medium or intermediate crudes, bituminous sands, and bituminous shale, and according to their density and API gravity are classified as shown in Table 1 (Aske., 2002, Rodgers et al., 2013, Barker., 1985).

### 1.2 Heavy crude oil main features

Heavy crude oils have a considerable complexity level due to their high content of asphaltenes, presence of heteroatoms, and organometallic such as Ni, V, Na, Ca, Fe. These features make them extremely viscous and cause significant difficulties and barriers both in the production chain and in

its study and understanding (Aske 2002; Rodgers et al., 2013; Barker 1985).

Because asphaltenes are a critical factor in the production trajectories and refining, a laboratory method was developed that allows quantifying crude oil into four families or fractions depending on their solubility and polarity: saturated (S), aromatic (A), resins (R), and the asphaltene fraction (A), known as S.A.R.A (Aske., 2002).

**Table 1.** Crude oils classification according to their density and API gravity.

Crude	Density (g/cm <sup>3</sup> )	°API
<b>Gas/condensates</b>	< 0,83	> 39
<b>Light</b>	0,83 - 0,87	31,1 - 39
<b>Medium</b>	0,87 - 0,92	22,3 - 31,1
<b>Heavy</b>	0,92 - 1,00	10,0 - 22,3
<b>Extra heavy</b>	> 1,00	< 10

Saturated or aliphatic hydrocarbons are nonpolar hydrocarbons that do not have double bonds, include linear and branched alkanes as well as cycloalkanes (naphthenes). Saturates are generally the fraction lighter crude oil. Aromatics are composed of highly unsaturated and polar molecules characterized by having at least a benzene ring in their structure. Higher molecular weight aromatics can fall into the resin or asphaltenes fraction (Aske 2002).

Asphaltenes are complex mixtures of a high and variable number of components. They have in their structure aromatic rings, heteroaromatic, and naphthenes, together with aliphatic chains and heteroatoms, mainly oxygen (O), nitrogen (N), and sulfur (S), in different functional groups like carboxylic acids, phenols, esters, amides, aromatic amines, ethers, among others. Asphaltenes contain metals such as nickel (Ni) and vanadium (V) in different organometallic compounds.

Asphaltenes and resins are the heaviest petroleum fractions. Asphaltenes are scattered in the continuous phase surrounded by the resins, according to the most accepted hypothesis. During processes production, asphaltenes tend to be associated with each other to form aggregates. These aggregates continue their association to form flocs or clots that can then precipitate. This precipitate is the major problem to be faced in the stages of processing and enhancement (Mansoori et al., 2004; Akbarzadeh et al., 2007; Ancheyta et al., 2013; Benyounes et al., 2017; Nguele et al., 2016; Dehaghani et al., 2017; Prakoso et al., 2017).

Resins fraction is considered an intermediate product in the asphaltenes generation. It is composed of polar molecules, which frequently contain heteroatoms such as N, O, and S. From an operational point of view is the fraction that solubilizes when the crude oil is dissolved in a light alkane such as pentane or heptane (Zhang et al., 2019; Guo et al., 2018).

## 2 Mesoscopic modeling

### 2.1 Dissipative Particle Dynamics (DPD)

The heavy crude oil model was built using the Dissipative Particle Dynamics technique (DPD) and the coarse-grained technique. DPD technique is based on the temporal evolution of the variables that describe the state of the particles, following Newton's equations, Eq. 1, (Maiti et al., 2004).

$$(1) \quad \frac{dr_i}{dt} = v_i, \quad \frac{dp_i}{dt} = \sum_{i \neq j} F_{ij}$$

The  $F_{ij}$  is interparticle forces, which are pairwise additive and act on the line joining between particle centers. These are central forces that satisfy Newton's third law, preserving the linear and angular momentum. These interparticle forces present three main contributions, conservative, random, and dissipative forces (Maiti et al., 2004):

$$(2) \quad F_{ij} = \sum_{i \neq j} (F_{ij}^C + F_{ij}^D + F_{ij}^R)$$

The first term in Eq. 2, corresponds to the conservative force, and it acts as a repulsive soft potential. The second term, defines the dissipative forces as the frictional forces that depend on the positions and relative velocities of particles. The third term, describes the random force necessary to maintain the system temperature. This research assumed the expressions raised in Silva et al (Silva et al., 2018).

In the heavy crude model generation, Hansen's experimental solubility parameters ( $\delta_{HSP}$ ), reported in the literature (Vegas 2014; Silva. 2015; Acevedo et al., 2004, 2010), were used to get Flory-Huggins values, basis on which the dpd-interaction parameters between the components of the systems were calculated. The methodology is the same that was followed by Silva et al (Silva et al., 2018).

### 2.2. Heavy crude oil mesoscopic modeling from S.A.R.A data

In this work, the coarse-grained technique was applied, making a super-grained of each fraction and elements that make up the mixtures studied, shown schematically in Fig. 1. In the proposed model, saturated and aromatics are represented by a dpd-particle identified as ML, defined as a maltene without resins. The resins mesoscopic model is represented by a dpd-particle identified as R. The asphaltene model is based on Acevedo et al proposal (Acevedo et al., 2004, 2010), which defines them as constituted by three groups, a resin sub-fraction (R2) and two asphaltenes sub-fractions called A1 and A2.

The main difference between A1 and A2 lies in its Hansen solubility parameter, where A1 has the highest value, followed by A2 and R,  $\delta_{HSP-R} < \delta_{HSP-A2} < \delta_{HSP-A1}$ . The asphaltene fraction was defined based on the two sub-fractions A1

and A2 each one represented and parameterized as a dpd-particle, according to the experimental solubility parameters. Models and dpd-interaction parameters calculation were performed from experimental data S.A.R.A, provided by the Venezuelan Institute of Technology for Petroleum, Los Teques, Miranda State, Venezuela (Intevep 2015-2017) and data reported in the literature (Dehaghani et al., 2017; Vegas., 2014; Silva., 2015; Acevedo et al., 2010).

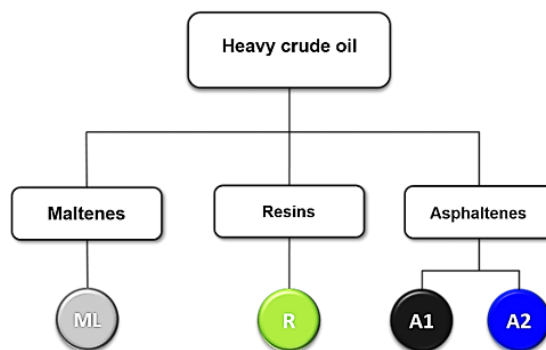


Fig. 1. Coarse-graining of a Heavy Crude Oil of the Orinoco Oil Belt from their S.A.R.A data

Table 2. Model parameters

General parameters	
$\Delta t$	0.01
$N_T$	100000
$N_{EQ}$	10000
T (°C)	35
Ensemble	nvt dpdv
Asphaltene system	
$N_{DPD}$	1501
A1	65%
A2	35%
Asphaltene and Resin system	
$N_{DPD}$	2403
ASF	85% (55% A1, 30% A2)
R	15%
Heavy Crude Oil model	
$N_{DPD}$	2435
ASF	20% (13% A1, 7% A2)
R	12%
ML	68%

$\Delta t$  is the time interval in dpd units,  $N_{EQ}$  is the iterations number to stabilize the system,  $N_T$  is the total iterations number,  $N_{DPD}$  total number of dpd-particles, and T the set temperature. A1, A2, R, and ML are the asphaltenes, resin and maltene fractions.

Three systems were generated and studied, one constituted by the asphaltenes, A1, A2, and the ASF system (A1-

A2). The second, formed by the asphaltene and resin fractions, ASF-R, and the third is the heavy crude oil, ASF-R-ML. All dynamics were carried out at a temperature of 35 °C, according to the conditions reported in *Table 2* and *Table 3*.

**Table 3.** Experimental Hansen solubility parameters ( $\delta_{HSP}$ ) of the Heavy Crude Oil (HCO) fractions (Silva., 2015, Acevedo et al., 2004, 2010).

Heavy Crude Oil fractions	$\delta_{HSP}$ (J/cm <sup>3</sup> ) <sup>1/2</sup>
A1	22,75
A2	21,30
R	18,35
ML	17,80

A1, A2, R, and ML are the asphaltenes, resin and maltene fractions.

Asphaltene system was defined by 65% dpd-particles of A1 type and 35% of the A2 fraction, according to experimental data reported by Acevedo et al (Acevedo et al., 2004, 2010, 2018), which indicate that sub-fraction A1 is the most abundant. The asphaltene and resin system is composed of 15% of the R fraction and 85% of the ASF fraction, which is made up of 65% of A1 subfraction and 35% of A2 subfraction. The heavy crude oil model (HCO) is constituted by 12% of the R fraction, 68% ML fraction, and 20% of ASF, which is composed in turn by 65% A1 and 35% A2.

All proportions were fixed following experimental and theoretical data reported for this type of crude (Vegas., 2014, Silva., 2015, Acevedo et al., 2004, 2010). The experimental  $\delta_{HSP}$  was used to calculate Flory-Huggins values ( $\chi$ ), with which the dpd-interaction parameters were obtained,  $a_{ij}$ , of the HCO fractions, reported in *Table 4*.

**Table 4.** Heavy crude oil dpd-interaction parameters.

DPD interactions parameters	$a_{ij}$
A1 - A2	25,64
A1 - R	30,88
A1 - ML	32,44
A2 - R	27,64
A2 - ML	28,72
R - ML	25,09

A1, A2, R, and ML are the asphaltenes, resin and maltene fractions.

### 3 Results and discussion

The construction and evaluation of a representative heavy crude model were carried out. In consequence, it began with the heavier components, the asphaltene fractions, A1, A2, and ASF (A1 and A2), which were evaluated through the behavior of ASF-nC7 and ASF-TOL mixtures. The next stage was incorporated the resin (R) and maltene (ML) fractions, this last the lightest fraction to obtain the heavy crude

oil model (HCO).

All systems were evaluated using the images of the dynamics, the density profiles calculation, and the evolution analysis of the interfacial tension values by varying the relative concentrations of the crude oil and its fractions with regard to the solvents.

#### 3.1 Model of heavy crude oil and its fractions

Starting with the assessment of the ASF fraction representative model, the dynamics carried out showed that A1 sub-fraction tends to form nano-aggregates surrounded by nano-aggregates of the A2 sub-fraction, uniformly distributed throughout the volume, as illustrated in *Fig. 2 (a)*. This is consistent with the density profile, *Fig. 3*, and images obtained by separating the system in the two sub-fractions, *Fig. 2 (b)* and *Fig. 2 (c)*, which show spaces evenly distributed throughout the volume that belongs to the place occupied by the other subfraction.

This result suggests a homogeneous mixture is generated at the nano-aggregates level and not at the molecular level. They are nano-aggregates of fractions mixed evenly, as suggested by the image taken of a nano aggregate from a mixture of 25% asphaltenes and 75% heptane, shown in *Fig. 2 (d)*.

The ASF-R system showed similar behavior to the ASF system, such that A1, A2, and R fractions formed nano-aggregates uniformly distributed throughout the volume, shown in *Fig. 4*. The density profile, *Fig. 5*, shows how the fractions' densities vary along X-axis, where A1 density increases where A2 and R densities decrease, the latter to a lesser degree, presenting a more regular distribution. This is in agreement with the most accepted conjecture that resins are stabilizing agents of asphaltenes in crude oil (Aske 2002; Mansoori et al., 2004; Guo et al., 2018; Vegas 2014).

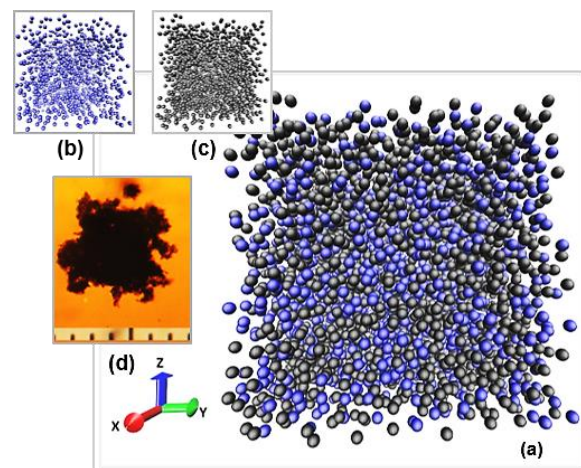


**Fig. 2.** (a) Asphaltene models. Dark gray and blue particles define the A1 and A2 subfractions. (b) Shows A1 and (c) A2 distribution. (d) Sample of 25% asphaltene and 75% heptane, taken in a 50X5.5 optical microscope.

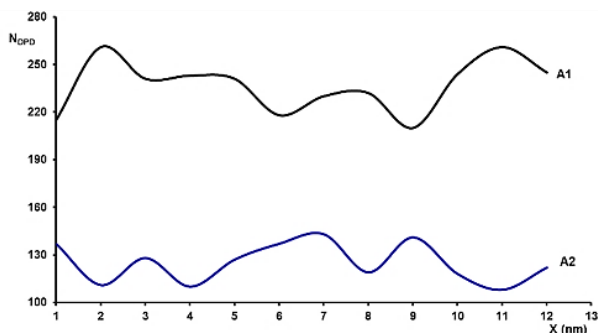


**Fig. 3.** Asphaltenes (A1 and A2) system density profile. NDPD is the number of particles of each species along the X-axis.

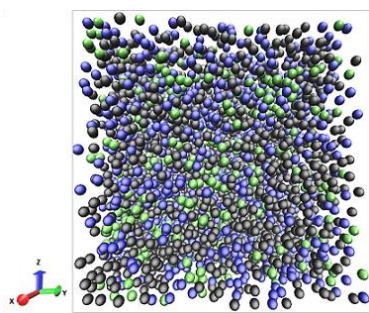


**Fig. 4.** Asphaltenes and resin system model. Dark gray, blue, and green particles define the asphaltenes A1, A2 subfractions, and the resin fraction.

In the HCO system, it was observed again that A1, A2, and R fractions form scattered nano-aggregates in the ML, which represents the crude oil least heavy fraction. With the ML inclusion, the asphaltene behavior in the crude oil is manifested as a colloidal suspension stabilized by the resins (Acevedo et al., 2010, 2018; Mozes et al., 2018; Salehi et al., 2017), illustrated in Fig. 6. This is compatible with the density profile distribution, Fig. 7, which records the variation of the relative concentration of the different heavy crude oil constituents along the X-axis.

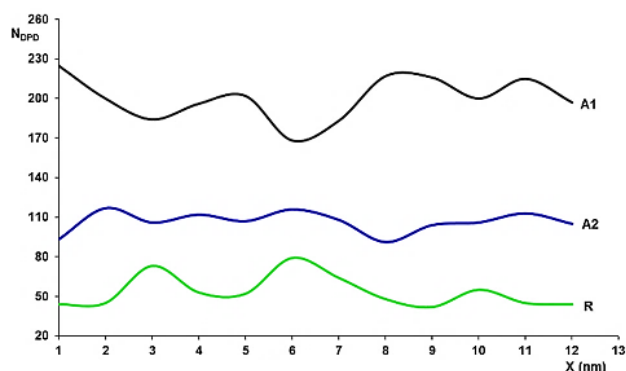


**Fig. 5.** Asphaltenes (A1, A2) and resin (R) system density profile. NDPD is the number of the particles of each species along the X-axis.

According to the results obtained in the approach of the ASF, ASF-R, and HCO models, it observed that A1 fraction

form nano-aggregates, surrounded by nano-aggregates of A2, stabilized by the R, suspended in the continuous phase of ML, which disperses these aggregates. The behavior of the modeled systems is consistent with the accepted hypothesis, which indicates that in a crude oil stable, such that no phase change has been initiated, asphaltenes are scattered in the lighter fractions, stabilized by the resins (Aske. 2002; Mansoori et al., 2004; Vegas 2014; Salehi et al., 2017).

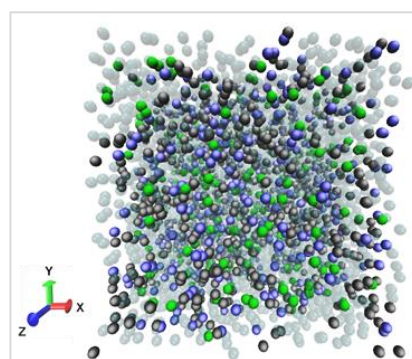


**Fig. 6.** Heavy crude oil model characteristic of Venezuela. Light gray, green, dark gray, and blue particles define the maltene (ML) and resin (R) fractions, and asphaltene subfractions (A1 and A2).

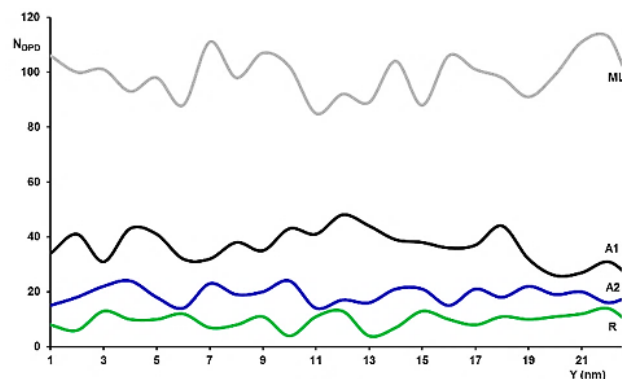


**Fig. 7.** Heavy crude oil model density profile. A1, A2, R, and ML are the asphaltene, resin and maltene fractions. NDPD is the number of the particles of each species along the Y-axis.

### 3.2. Interfacial tension estimation of the asphaltene system in heptane and toluene mixtures at different concentrations.

Following the methodology set out, 25 types of ASF mixing with nC7 and TOL were modeled and studied. In the approach of the systems, the  $\delta_{HSP}$  experimental values published were used (Acevedo et al., 2010; Levin et al., 2008; Majumdar et al., 2014) of  $15.30 \text{ (J/cm}^3\text{)}^{1/2}$  for nC7 and  $18.04 \text{ (J/cm}^3\text{)}^{1/2}$  for TOL.

These values were used to  $\chi$  calculations, which were later used to obtain the dpd-interaction parameters of 41.86 for A1-nC7, 31.40 for A1-TOL, 35.93 for A2-nC7, and 27.99 for A2-TOL.

For heptane mixtures, DPD dynamics of 10 different concentrations were performed for each system, A1-nC7, A2-nC7, and ASF-nC7. It was started with a mixture of 95% asphaltene concentration (A1, A2, or ASF) regarding 5% nC7, reported as 95/5. It was continued decreasing the asphaltene percentage and increasing the nC7 percentage as follows: 95/5, 90/10, 80/20, 70/30, 60/40, 50/50, 40/60, 30/70, 20/80, 10/90.

The expected behavior is that these fractions segregate in relation to the nC7 as their concentration increases. This is manifest in results reported in Fig. 8, which are consistent with the experimental IFT values evolution in this type of mixture, under similar conditions (Mansoori et al., 2004).

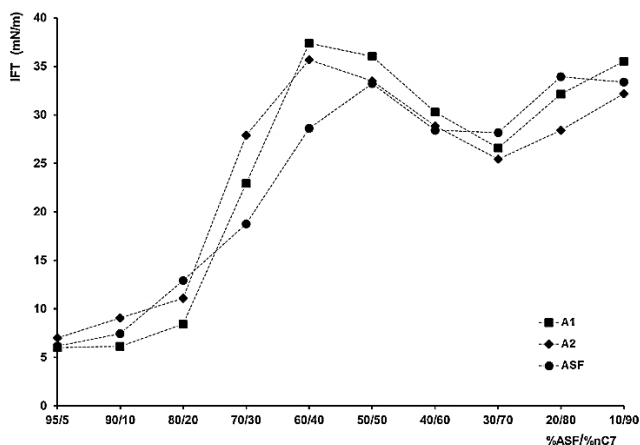


Fig. 8. Interfacial Tension (IFT) estimated values of asphaltenes (ASF) with heptane (nC7) mixtures, varying the relative concentrations.

Initially, for very low nC7 concentrations (5% and 10%), mixtures have an IFT ranging from 6.00 mN/m to 7.44 mN/m, presenting the ASF mixture, IFT average values of 6.18 mN/m and 7.44 mN/m for 5% and 10% of heptane. When the heptane concentration was increased to 20%, there was a moderate increase in the IFT values. For this concentration, the mixture presented an IFT value of 12.91 mN/m.

For concentrations higher than 20%, there was observed a significant increase of the IFT values, reaching their highest values for A1-nC7 of 37.37 mN/m and A2-nC7 of 35.70 mN/m, at 40% of nC7 concentration, and for the ASF-nC7 system a maximum IFT of 33.93 mN/m, at 80% nC7 concentration. The increase, decrease, and new IFT increase on asphaltene-heptane mixtures is attributed to a change in the aggregation and distribution of A1 aggregates with respect to A2 and A1-A2 concerning the solvent. Mixtures A1, A2, and ASF with nC7 follow the same trend to the extent that the concentration of the solvent is varied.

The asphaltene concentration impact in organic solvents is of great interest due to the formation of two or more phases, differentiated by their micelle content richness (CMC) (Nguele et al., 2016; Dehaghani et al., 2017; Acevedo et al., 2018; Evdokimov et al., 2016; Svalova et al., 2017). In

this sense, toluene was selected to evaluate models and methodology used, through interfacial tension evolution in the systems. For this purpose, 15 ASF-TOL systems were designed at different concentrations, set as 2.2/97.8, 2.4/97.6, 2.6/97.4, 2.8/97.2, 3.0/97.0, 3.4/96.6, 4.5/95.5, 5.5/94.5, 6.0/94.0, 7.0/93.0, 8.0/92.0, 9.0/91.1, 12.0/88.0, 16.0/84.0, 20.0/80.0. It was started from a concentration of 2.2% ASF regarding 97.8% TOL and the ASF concentration was increased as the TOL volume decreased.

Theoretical IFT evolution results reported in Fig. 9 show that: (a) For the minimum asphaltene concentration of 2.2%, was obtained an IFT of 27.99 mN/m. (b) The IFT decreased as the ASF concentration increased regarding TOL, until reaching a minimum IFT value of 25.28 mN/m, for 2.8% ASF concentration. (c) By continuing to increase the ASF content relative to the solvent, a perceptible IFT value increase occurred, reaching a maximum value of 29.35 mN/m at 5.5% ASF concentration. (d) From the previous point begins a new IFT values decrease, which reaches a second minimum value of 28.06 mN/m at 7% ASF concentration. (e) Finally, for ASF concentrations greater than 7%, the IFT values increase, until stabilized from 12% ASF concentration.

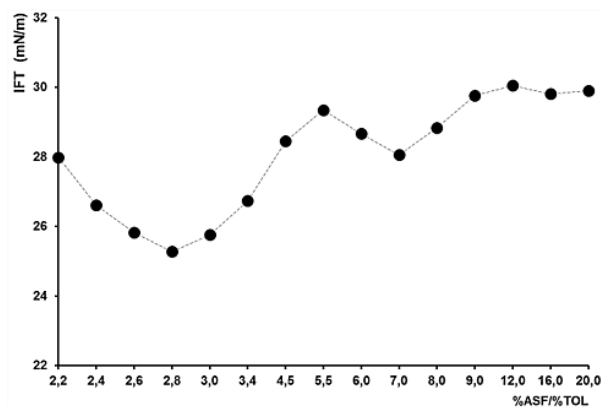


Fig. 9. Interfacial Tension (IFT) estimated values of asphaltene (ASF) with toluene (TOL) mixtures, varying the relative concentrations.

From the previous behavior can be deduced that at the beginning of the increase in the ASF concentration with respect to the TOL, (a) and (b), this aromatic solvent is able to solubilize the ASF completely. For 2.8% ASF concentration (b), a point of critical micelle concentration is reached (CMC). The system begins a phase transition (c), the separation of asphaltene in small aggregates, scattered like amorphous nano-drops in the solvent, which as they are added, their size increases.

By continuing to increase the ASF concentration, there is a second IFT values decline (d), suggesting that there is a re-arrangement of these aggregates, increasing their dispersion in the solvent, this being another point of CMC. From this concentration, an IFT values increase starts again (e), which is stabilized from ASF concentrations higher than

12%.

It must be taken into account that these results correspond to a theoretical study carried out with small systems, so they are not conclusive. It is necessary to expand the research, combining more extensive theoretical analysis with experimental tests and verifications.

### 3.3. Interfacial tension estimation in heavy crude oil and saline water mixtures at different concentrations of salt.

The brines injection at different salinity concentrations is one of the EOR methods applied to reduce the interfacial tension forces. Nowadays, the mechanisms behind this type of process are still a subject of study. In this sense, heavy crudes from Venezuela, particularly those in the Orinoco Oil Belt, have as one of their relevant characteristics a high content of salts in their formation water, which affects the recovery methods and raises costs in the transportation and refining processes. It should be noted that few experimental data similar to the study carried out are reported, therefore, little information is available (Ayirala et al., 2018, Lashkarbolooki et al., 2016, Israelachvili et al., 2017, Mehraban et al., 2021).

In consequence, it was decided to include two types of mixtures of heavy crude oil with saline water, one constituted by HCO with NaCl brines, abbreviated as S1 salt, and another formed by HCO with CaCl<sub>2</sub> brines, abbreviated as S2 salt. For these systems, the calculated  $a_{ij}$  parameters were 49.34 for the A1-W interaction, 52.22 for A2-W, 36.45 for the A1-brine, and 38.45 for A2-brine interaction. All systems were studied at 35 °C, with 30% HCO and 70% saline water. It applied the methodology described in Silva et al (Silva et al., 2018) and the experimental approach proposed by Shahab and collaborators (Ayatollahi et al., 2014).

Similar systems were evaluated (Ayatollahi et al., 2014), where salt concentrations in water (S1/W or S2/W) were set as 2/98, 4/96, 6/94, 8/92, 10/90, 12/88, 14/86, 16/84, 18/82, 20/80, 25/75, such that 2/98 involves 2% S1 or S2 salt and 98% water. The asphaltenes used in the Interfacial Tension experimental estimation were obtained from the Carabobo oil field in Venezuela, described in *Appendix A*.

In the results, shown in *Fig. 10* and *Fig. 11*, starting from a 2% salt concentration, the IFT decreased as the salt concentration increased until reaching 10% and 12%, for theoretical and experimental S1 concentration, and 8% and 10% for theoretical and experimental S2 concentration. Then, from these values, IFT increased as salt concentrations increased. At maximum salt saturation of 25% was obtained theoretical and experimental IFT values of 22.60 mN/m and 18.90 mN/m for S1, and 26.86 mN/m, 22.30 mN/m for S2 were.

These results suggest that in the mixtures studied at low salt concentrations, the ASF and R in crude oil acts as a surfactant that dominates the effect of salt, which causes the IFT to decrease as the salinity of the medium increases. Then, when reaching a certain point of salt saturation, the ASF and R interact less with the interface, showing more similar to

crude oil, such that the heavier fractions, A1 and A2, tend to aggregate.

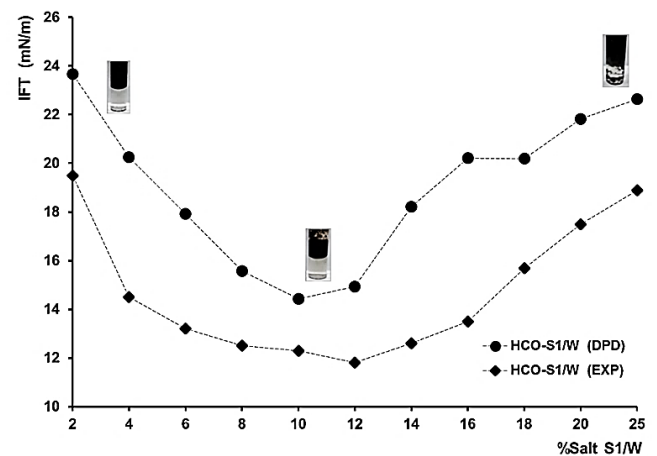


**Fig. 10.** Interfacial Tension (IFT) values of mixtures of a Heavy Crude Oil (HCO) with brine of NaCl (S1), varying the salt in water (W) concentrations. Experimental results (EXP).

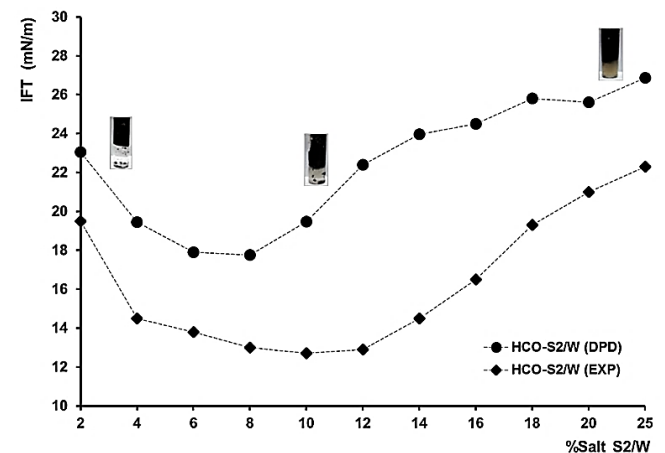


**Fig. 11.** Interfacial Tension (IFT) values of mixtures of a Heavy Crude Oil (HCO) with brine of CaCl<sub>2</sub> (S2), varying the salt in water (W) concentrations. Experimental results (EXP).

Even though brine tends to penetrate the crude oil interstices, the IFT increases with increasing salt concentration, illustrated in the images from the dynamics of the systems, *Fig. 12* and *Fig. 14*. On the other hand, a difference is noted in the saline water absorption regarding the type of salt and their concentration, as seen in the density profiles presented in *Fig. 13*, *Fig. 15*, and the images from the dynamics.

For HCO-S1 mixtures, the saline water began to be absorbed as the salt concentration increased, which caused the disperse of oil and formed an emulsion of oil in water, *Fig. 12*. Similar behavior was obtained with HCO-S2 systems. As the salt concentration increased, the penetration of saline wa-

ter increased, but in this case, this occurred to a greater degree, *Fig. 14*. For a maximum salt concentration of 25%, the crude oil expanded significantly, and an emulsion of crude oil in water was formed, shown in *Fig. 13* and *Fig. 15*. It is noteworthy that the HCO-S2 systems' IFT values, both theoretical and those measured experimentally, were higher than those presented by the HCO-S1 systems were.

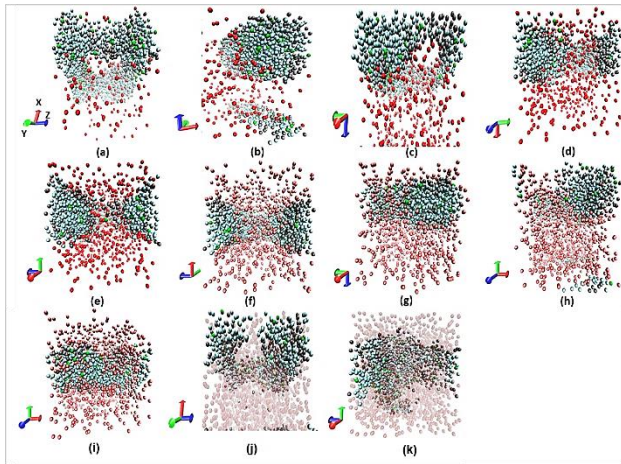


**Fig. 12.** Mixtures of Heavy Crude Oil (HCO) and brine of NaCl at different salt in water concentrations: (a) 2/98, (b) 4/96, (c) 6/94, (d) 8/92, (e) 10/90, (f) 12/88, (g) 14/86, (h) 16/84, (i) 18/82, (j) 20/80, (k) 25/65. Blue, green, and gray particles define maltene, resin, and asphaltene fractions, and dark and light red the salt, and the background represents the W volume.

For the results presented, both theoretical and experimental, so far there is no similar information, in detail, with which these results can be contrasted. It is known, from an operational point of view, that they follow the trend of non-systematic measurements that have been carried out on similar mixtures in the field.

In this sense, it is conjectured the behavior of the IFT to occur because as saline water occupies oil crude interstices, it generates an aggregates compaction with respect to the brine which causes an IFT increases towards these interfaces. In the case of the HCO-S1 mixtures, this salt tends to produce more stable emulsions with less compact aggregates, producing lower IFT values. On the other hand, the theoretically estimated values closely follow and reproduce the same trend that experimental values, although they were consistently higher than those measured experimentally for both systems were.

#### 3.4. Interfacial tension estimation in heavy crude oil and solvents mixtures at different concentration

Finally, nine mixtures of HCO with the solvents nitrobenzene, pyridine, cyclohexanone, toluene, benzene, oleic acid, methanol, pentane, and heptane were studied, abbreviated as NTRBZ, PRD, CHXN, TOL, BENZ, ACO, MTN, nC5, nC7.

The dpd-interaction parameters are reported in Appendix B. A study of this type of mixture was carried out due to its relevance in the oil industry and to evaluate the proposed models. All systems were built according to *Tables 2, 3, 4,* and *Table A of Appendix B* data in a proportion of 30% HCO compared to 70% solvent.

The solvents were selected from the best solvent, which particularly solubilizes A1 and A2 heavy fractions, to the worst solvents, which do not solubilize these fractions and induce their precipitation, based on reported experimental data (Vegas 2014; Acevedo et al., 2004, 2010, 2018).

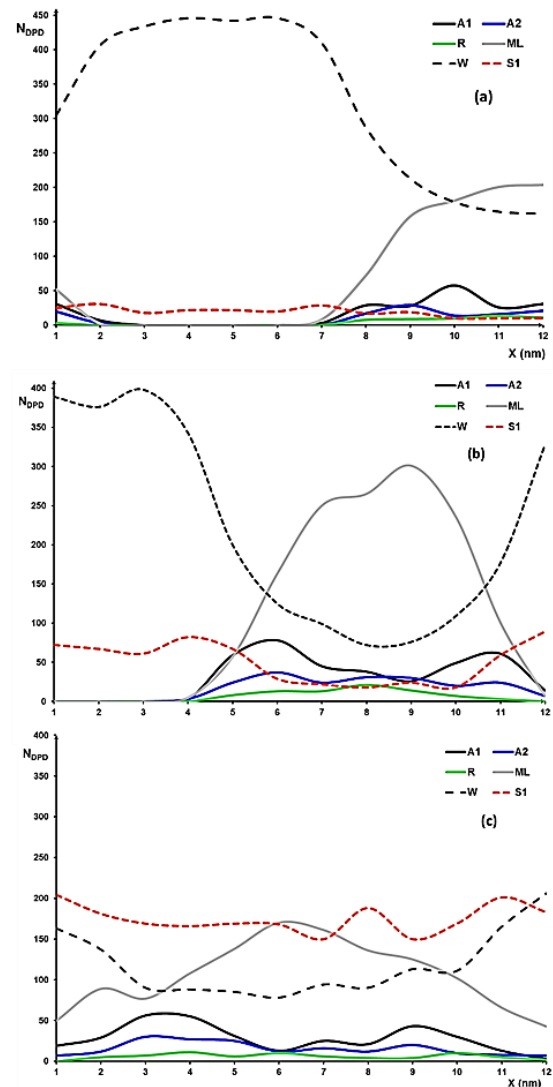


**Fig. 13.** Density profile of mixtures of a Heavy Crude Oil (HCO) and brine of NaCl at different salt in water concentrations: (a) 4/96, (b) 12/88, (c) 20/80, (d) 25/75. A1, A2, R, ML represent asphaltene, resin, and maltene fractions. NDPD is the number of the particles of each species and X the cutting axis.



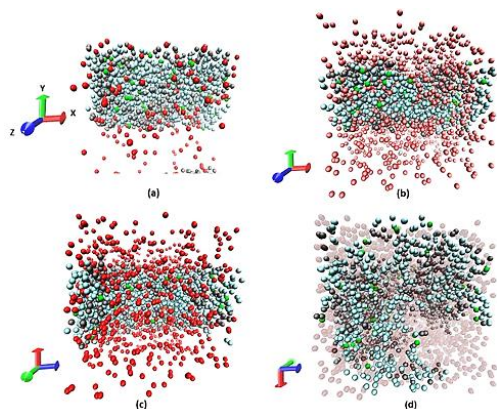


**Fig. 14.** Mixtures of Heavy Crude Oil (HCO) and brine of CaCl<sub>2</sub> at different salt in water concentrations: (a) 4/96, (b) 12/88, (c) 20/80, (d) 25/75. Blue, green, and gray particles define maltene, resin, and asphaltene fractions, the dark and light red the salt, and the background the water volume.

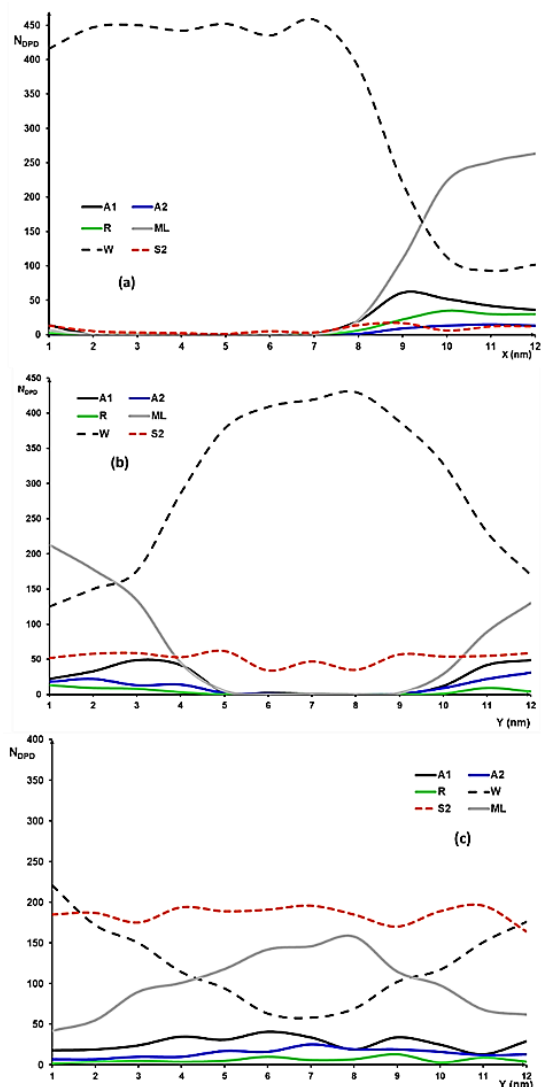


**Fig. 15.** Density profile of mixtures of a Heavy Crude Oil (HCO) and brine of CaCl<sub>2</sub> at different salt in water concentrations: (a) 4/96, (b) 12/88, (c)

20/80, (d) 25/75. A1, A2, R, ML represent asphaltenes, resin, and maltene fractions. NDPD is the number of the particles of each species and Y the cutting axis.

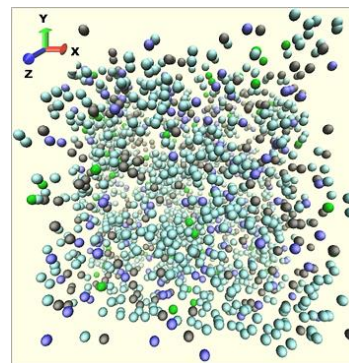


**Fig. 16.** Model of a Heavy Crude Oil and Nitrobenzene mixture. The light blue, green, dark blue, and gray particles define the maltene and resin fractions, and A1-A2 asphaltene subfractions. The background represents the nitrobenzene volume.

In this sense, the best performance was presented by the NTRBC, who solubilized all crude oil fractions, shown in Fig. 16, where it is observed that the crude oil components are dispersed by this solvent, agree to the experimental behavior reported (Vegas., 2014, Acevedo et al., 2004, 2010, 2018), and with the lowest IFT value of 14.56 mN/m, shown in Fig. 17.

In descending order, according to the ability to solubilize crude oil, in particular asphaltenes, it was found that pyridine was the second-best solvent, followed by cyclohexanone, toluene, benzene, and oleic acid, which is reflected by the IFT increase in that same direction, shown in Fig. 17. These results are in line with the laboratory test measurement results observed on similar mixtures under alike conditions (Intevp., 2015-2017).

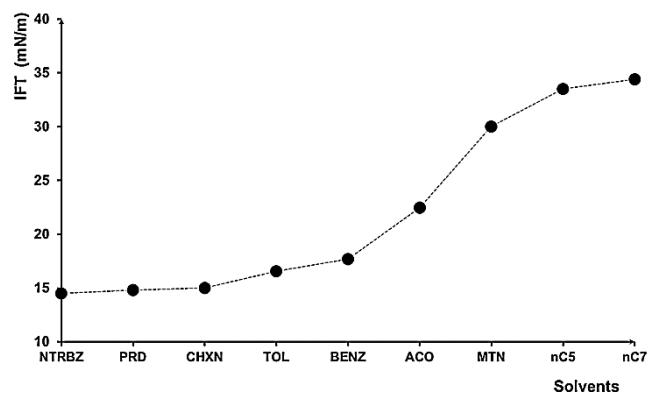


**Fig. 17.** Estimated Interfacial Tension values (IFT) of mixtures of a Heavy Crude Oil with the solvents: nitrobenzene (NTRBZ), pyridine (PRD), cyclohexanone (CHXN), toluene (TOL), benzene (BENZ), oleic acid (ACO), methanol (MTN), pentane (nC5), and heptane (nC7).

In descending order, according to their ability to solu-

bilize the crude oil, the worst solvents were methanol, n-pentane, and n-heptane. These solvents produced ASF segregation and precipitation, partial solubilization of the R fraction, and ML fraction solubilization. The asphaltenes phase separation was more pronounced with nC5 and nC7 solvents. Fig. 18, from the dynamics, shows how the asphaltene fraction (A1 and A2) precipitates, while the R and ML fraction are highly solubilized.

The results trend for the worst solvents is in agreement with the operational definition of asphaltenes and resin fractions, as already mentioned, according to which asphaltenes are insoluble in these solvents, while the resins present different levels of solubility.

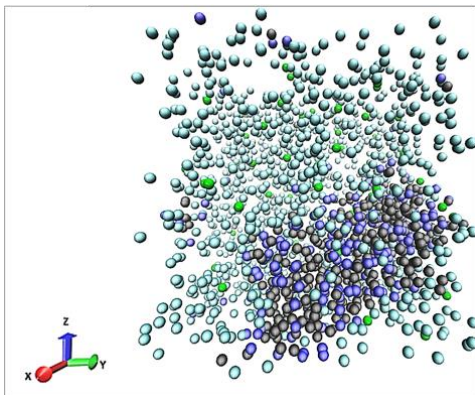


**Fig. 18.** Model of a Heavy Crude Oil and Heptane mixture. The light blue, green, dark blue, and gray particles, define the maltene and resin fractions, and the A1-A2 asphaltenes subfractions. The background represents the nC7 volume.

These results are at the same time confirmed by the interfacial tension values increasing trend, Fig. 17, whose highest values were obtained for HCO-nC5 and HCO-nC7 mixtures, which indicates the low affinity of these solvents with crude oil.

As with the crude and brine systems, it was verified that these values and systems follow the trend, and the behavior observed in similar mixtures in the field (Intevp., 2015-2017). The comparison of this type of data is complex due to the difficulties that arise in the interfacial tension measurement in heavy and extra heavy crude oils. Therefore, obtaining these values by methods such as the one proposed is significant in understanding this type of system.

#### 4 Acknowledgments

My warmest thanks to Aleixandre Chirinos from the Analytical Chemistry Laboratory of Intevp, Venezuela, for their suggestions, clarifications, and support for this research work.

#### 5 Conclusions

A heavy crude model characteristic from Venezuela is

proposed, modeled applying dissipative particle dynamics technique and the coarse-grain technic, parameterized from experimental S.A.R.A data.

The heavy crude model showed that fraction A1 tends to form nano-aggregates, surrounded by nano-aggregates of A2, stabilized by the resin, suspended in the continuous phase of maltene, which tends to disperse these aggregates. The results indicate that components are distributed as a homogeneous mixture at the nano-aggregate level and not at the molecular level.

The models of asphaltenes-heptane mixtures showed the expected segregation behavior as the heptane concentration increased, which is reflected in continuous interfacial tension increase. The interfacial tension increase, decrease, and new increase are attributed to a change in the aggregation and distribution of the nano-aggregates of A1 regarding A2 and A1-A2 regarding heptane.

In the interfacial tension study on the asphaltenes-toluene systems, for low asphaltene values concentration, it was found that the aromatic solvent completely solubilized the asphaltene. Upon around 2.8% asphaltene content, a critical micelle concentration point was produced, giving place to a phase transition, the asphaltenes separation into small aggregates, dispersed in the solvent. Around 7% asphaltene concentration, it was produced a second critical micelle concentration point, which seems to indicate that a rearrangement of these aggregates occurs, increasing their dispersion in the solvent. The asphaltene content increase was accompanied by an interfacial tension increase, which tended to stabilize from 12% asphaltene concentration.

The heavy crude oil with saline water of sodium chloride and calcium chloride results showed that at low salt concentrations, the asphaltenes and resin act as a surfactant that dominates the effect of the salt, which causes the interfacial tension to decrease as the salinity of the medium increases. Upon reaching a certain salt saturation point, asphaltenes and resins interact less with the interface, showing more similarity to crude oil, such that the heavier fractions, A1 and A2 tend to aggregate, which drives the continuous interfacial tension increase until the emulsion stabilizes. In such a way that, at low salt, concentrations arose well-defined interfaces and from a critical salt concentration occurred a crude oil in water emulsions. Additionally, it was observed that this behavior was more pronounced in the sodium chloride brines.

Finally, nine mixtures of heavy crude oils with the solvents nitrobenzene, pyridine, cyclohexanone, toluene, benzene, oleic acid, methanol, pentane, and heptane were studied, in descending order according to their ability to solubilize crude oil, in particular asphaltenes. According to their ability to solubilize crude oil, nitrobenzene presented the best performance, followed by pyridine, cyclohexanone, and toluene. The worst solvents were methanol, n-pentane, and n-heptane which generated segregation and precipitation of asphaltenes, partial solubilization of the resin, and solubilization of the maltene fraction. These results are reflected in the increase of the interfacial tension.

The interfacial tension values calculated, reproduce the trends and behaviors reported for these systems under similar conditions. Acquiring this type of data in a detailed and systematic way is difficult and expensive due to the intrinsic complexities of crude oil according to the reservoir characteristics and exploitation method. Therefore, getting this type of data, using the power of the computational methods in combination with experimental databases, represents an essential contribution to the generation of knowledge in the study of this type of system.

## References

- Ancheyta J et al. (2013). Chemical Characterization of Asphaltenes from Various Crude Oils. *Fuel Processing Technology* 106 (febrero), pp. 734-38. <https://doi.org/10.1016/j.fuproc.2012.10.009>.
- Ayrala S C et al. (2018). Effects of Salinity and Individual Water Ions on Crude Oil-Water Interface Physicochemical Interactions at Elevated Temperature. *SPE*. <https://doi.org/10.2118/190387-MS>.
- Ayatollahi S et al. (2014). Toward Mechanistic Understanding of Heavy Crude Oil/Brine Interfacial Tension: The Roles of Salinity, Temperature and Pressure. *Fluid Phase Equilibria* 375, pp. 191-200. <https://doi.org/10.1016/j.fluid.2014.04.017>.
- Benyounes K et al. (2017). Removal and Prevention of Asphaltene Deposition during Oil Production: A Literature Review. *Journal of Petroleum Science and Engineering* 158, pp. 351-60. <https://doi.org/10.1016/j.petrol.2017.08.062>.
- Dehaghani A H S, and Badizad M H. (2017). Inhibiting Asphaltene Precipitation from Iranian Crude Oil Using Various Dispersants: Experimental Investigation through Viscometry and Thermodynamic Modelling. *Fluid Phase Equilibria* 442, pp. 104-18. <https://doi.org/10.1016/j.fluid.2017.03.020>.
- Em Karniadakis G et al. (2014). Accelerating Dissipative Particle Dynamics Simulations on GPUs: Algorithms, Numerics and Applications. *Computer Physics Communications* 185 (11), pp. 2809-22. <https://doi.org/10.1016/j.cpc.2014.06.015>.
- Evdokimov I N and Fesan, A, A. (2016). Multi- Evdokimov, I, N. Step Formation of Asphaltene Colloids in Dilute Solutions. *Colloids and Surfaces A: Physicochemical and Engineering Aspects* 492, pp. 170-80. <https://doi.org/10.1016/j.colsurfa.2015.11.072>.
- Fang S et al. (2017). Mesoscopic Probes in Asphaltenes Nanoaggregate Structure: From Perpendicular to Paralleled Orientation at the Water-in-Oil Emulsions Interface. *RSC Advances* 7 (61), pp. 38193-203. <https://doi.org/10.1039/C7RA06717H>.
- Guo A et al. (2018). Peptizing Effect of the Native Heavy Resin Fraction on Asphaltenes. *Energy & Fuels* 32 (3), pp. 3380-90. <https://doi.org/10.1021/acs.energyfuels.8b00208>.
- Israelachvili J N et al. (2017). Effects of Salinity on Oil Recovery (the “Dilution Effect”): Experimental and Theoretical Studies of Crude Oil/Brine/Carbonate Surface Restructuring and Associated Physicochemical Interactions. *Energy & Fuels* 31 (9), pp. 8925-41. <https://doi.org/10.1021/acs.energyfuels.7b00869>.
- Kamran A et al. (2007). Los asfaltenos: Problemáticos pero ricos en potencial. *Schlumberger*, pp. 1-24.
- Lashkarbolooki M, Riazi M and Ayatollahi S. (2016). Investigation of Effects of Salinity, Temperature, Pressure, and Crude Oil Type on the Dynamic Interfacial Tensions. *Chemical Engineering Research and Design* 115 (noviembre), pp. 53-65. <https://doi.org/10.1016/j.cherd.2016.09.020>.
- Levin M and Per Redelius. (2008). Determination of Three-Dimensional Solubility Parameters and Solubility Spheres for Naphthenic Mineral Oils. *Energy & Fuels* 22 (5), pp. 3395-3401. <https://doi.org/10.1021/ef800256u>.
- Li Y et al. (2013). Dissipative Particle Dynamics Simulation on the Properties of the Oil/Water/Surfactant System in the Absence and Presence of Polymer. *Molecular Simulation* 39 (4), pp. 299-308. <https://doi.org/10.1080/08927022.2012.724173>.
- Maiti A and McGrother S. (2004). Bead-bead Interaction Parameters in Dissipative Particle Dynamics: Relation to Bead-Size, Solubility Parameter, and Surface Tension. *The Journal of Chemical Physics* 120 (3), pp. 1594-1601. <https://doi.org/10.1063/1.1630294>.
- Majumdar S et al. (2014). Estimation of Interfacial Tension for Immiscible and Partially Miscible Liquid Systems by Dissipative Particle Dynamics. *Chemical Physics Letters* 600, pp. 62-67. <https://doi.org/10.1016/j.cplett.2014.03.061>.
- Mehraban M F et al. (2021). Debunking the Impact of Salinity on Crude Oil/Water Interfacial Tension. *Energy & Fuels* 35 (5), pp. 3766-79. <https://doi.org/10.1021/acs.energyfuels.0c03411>.
- Modarress H et al. (2016). Self-Accumulation of Uncharged Polyaromatic Surfactants at Crude Oil-Water Interface: A Mesoscopic DPD Study. *Energy & Fuels* 30 (8), pp. 6626-39. <https://doi.org/10.1021/acs.energyfuels.6b00254>.
- Mousavi-Dehghani S, A., Riazi, M, R., Vafaie-Sefti, M and Mansoori, G, A. (2004). An Analysis of Methods for Determination of Onsets of Asphaltene Phase Separations. *Journal of Petroleum Science and Engineering* 42 (2-4), pp. 145-56. <https://doi.org/10.1016/j.petrol.2003.12.007>.
- Mozes E et al. (2018). Behavior of Asphaltene and Asphaltene Fractions Films on a Langmuir-Blodgett Trough and Its Relationship with Proposed Molecular Structures. *Petroleum Science and Technology* 36 (18), pp. 1490-96. <https://doi.org/10.1080/10916466.2018.1479422>.
- Narve A. (2002). Characterisation of Crude Oil Components, Asphaltene Aggregation and Emulsion Stability by Means of Near Infrared Spectroscopy and Multivariate

- Analysis. Doctoral thesis, Trondheim, Norwegian: Norwegian University of Science and Technology. <https://www.semanticscholar.org/paper/Characterisation-of-crude-oil-components%2C-and-by-of-Aske/801e7ec595664b5ac7ebcaa4fb53d9ff52c810e4>.
- Nguele R et al. (2016). Asphaltene Aggregation in Crude Oils during Supercritical Gas Injection. *Energy & Fuels* 30 (2), pp. 1266-78. <https://doi.org/10.1021/acs.energyfuels.5b02903>.
- Prakoso A A et al. (2017). A Mechanistic Understanding of Asphaltenes Precipitation From Varying-Saturate-Concentration Perspectives. *SPE Production & Operations* 32 (01), pp. 86-98. <https://doi.org/10.2118/177280-PA>.
- Sabirgalieva N et al. (2017). DPD simulation of surface wettability alteration by added water-soluble surfactant in the presence of indigenous oil-soluble surfactant. *Chemical Engineering Transactions* 57, pp. 1489-94. <https://doi.org/10.3303/CET1757249>.
- Salehi M et al. (2017). The Relationship between SARA Fractions and Crude Oil Stability. *Egyptian Journal of Petroleum* 26 (1), pp. 209-13. <https://doi.org/10.1016/j.ejpe.2016.04.002>.
- Silva C del V. (2015). A Mesoscopic Model for an Asphaltene and Complex Mixtures of Asphaltenes. *Petroleum Science and Technology* 33 (7), pp. 839-45. <https://doi.org/10.1080/10916466.2014.986278>.
- Silva C del V. (2018). Estimation of Interfacial Tension in Mixtures of Linear Hydrocarbons and Immiscible Organic Liquids with Water by Dissipative Particle Dynamics (DPD). *International Journal of Fluid Mechanics & Thermal Sciences* 4 (1), pp. 1. <https://doi.org/10.11648/j.ijfmts.20180401.11>.
- Sócrates A et al. (2018). Suppression of Phase Separation as a Hypothesis to Account for Nuclei or Nanoaggregate Formation by Asphaltenes in Toluene. *Energy & Fuels* 32 (6), pp. 6669-77. <https://doi.org/10.1021/acs.energyfuels.8b00949>.
- Sócrates A et al. (2010). Investigation of Physical Chemistry Properties of Asphaltenes Using Solubility Parameters of Asphaltenes and Their Fractions A1 and A2. *Energy & Fuels* 24 (11), pp. 5921-33. <https://doi.org/10.1021/ef1005786>.
- Sócrates A et al. (2004). Structural Analysis of Soluble and Insoluble Fractions of Asphaltenes Isolated Using the PNP Method. Relation between Asphaltene Structure and Solubility. *Energy & Fuels* 18 (2), pp. 305-11. <https://doi.org/10.1021/ef030065y>.
- Svalova A et al. (2017). Determination of Asphaltene Critical Nanoaggregate Concentration Region Using Ultrasound Velocity Measurements. *Scientific Reports* 7 (1), pp. 16125. <https://doi.org/10.1038/s41598-017-16294-5>.
- Vegas K G. (2014). Factores moleculares y coloidales de los asfaltenos: su estudio mediante parametros de solubilidad, captura de porfirinas matalicas y punto de fusion. Doctoral thesis, Caracas, Venezuela: Université Claude Bernard - Lyon I; Universidad central de Venezuela.
- Xu J et al. (2014). The Aggregation and Diffusion of Asphaltenes Studied by GPU-Accelerated Dissipative Particle Dynamics. *Computer Physics Communications* 185 (12), pp. 3069-78. <https://doi.org/10.1016/j.cpc.2014.07.017>.
- Xu J et al. (2015). Dissipative Particle Dynamics Simulation on the Rheological Properties of Heavy Crude Oil. *Molecular Physics* 113 (21), pp. 3325-35. <https://doi.org/10.1080/00268976.2015.1021396>.
- Zhang J et al. (2019). Influence of Resins on Crystallization and Gelation of Waxy Oils. *Energy & Fuels* 33 (1), pp. 185-96. <https://doi.org/10.1021/acs.energyfuels.8b03488>.
- Zhang L et al. (2019). Mesoscale Simulation for Heavy Petroleum System Using Structural Unit and Dissipative Particle Dynamics (SU-DPD) Frameworks. *Energy & Fuels* 33 (2), pp. 1049-60. <https://doi.org/10.1021/acs.energyfuels.8b04082>.
- Zhiqiang B and Guo H. (2013). Interfacial Properties and Phase Transitions in Ternary Symmetric Homopolymer-Copolymer Blends: A Dissipative Particle Dynamics Study. *Polymer* 54 (8), pp. 2146-57. <https://doi.org/10.1016/j.polymer.2013.02.011>.

## Appendix A

The asphaltenes separation process used to experimental interfacial tension calculation:

- Asphaltenes used in the interfacial tension (IFT) experimental estimation were obtained from the Carabobo oil field in Venezuela. For this purpose, the crude was dissolved in heptane to solubilize the saturated, aromatic compounds and resins. The insoluble fraction obtained was purified, removing the resins. Finally, the separated asphaltenes were dried. The whole process was carried out according to the methodology indicated below:
  - Asphaltenes precipitation: It was started from a given volume of crude oil, which was heated to 60 °C. Then, heptane was added, with gentle agitation, in a relationship 1:30 of HCO:n-C7. This mixture was stirred for 6 hours and left to stand for 24 hours. Afterward, the insoluble part was separated by gravity filtration. The precipitate obtained required a purification step to remove the resins that had co-precipitated with the asphaltenes.
  - Asphaltenes Purification: Resins were extracted by a Soxhlet system with consecutive heptane washes until observing solvent transparency. Once washed the asphaltenes, were placed in a reflux system with heptane for 8 hours to perform the final removal of the resins.
  - Asphaltenes Drying: The solid obtained in the previous step was dried on a stove at 100 °C and 120 °C

to remove heptane traces that could contain the asphaltenes. The solid was stored in glass vials until later use.

• The experimental interfacial tension was estimated using a Spinning Drop SVT 20N tensiometer, specifically designed to measure extremely low interfacial tensions. Enclosed inside a glass capillary, at speeds up to 20,000 rpm, the drops are kept within the field of vision by the tilt of the measuring cell and the control of the position of the camera. Interfacial tensions were calculated based on the contours of the drops, the predefined speed increments, and the sinusoidal velocity variations of relaxation measures.

• The IFT experimental measurements were carried out for the Heavy Crude Oil and brine of NaCl and CaCl<sub>2</sub> systems. Thereby, they carried out two separate runs of 150 measurements were performed for each point, reporting as interfacial tension experimental (EXP) the average of these measurements, taken from the moment when both the drop and the temperature have equilibrated, with a temperature range of  $35 \pm 0.5$  °C.

## Appendix B

**Table A.** Interaction parameters  $a_{ij}$  of the asphaltenes (A1 and A2), resin (R), and maltene (ML) fractions with the selected solvents: nitrobenzene (NTRBZ), pyridine (PRD), cyclohexanone (CHXN), toluene (TOL), benzene (BENZ), oleic acid (ACO), methanol (MTN), pentane (nC5), and heptane (nC7).

DPD-interactions parameters HCO - solvents	$a_{ij}$
A1-NTRBC	25,11
A1-PRD	25,30
A1-CHXN	28,09
A1-TOL	31,40
A1-BENZ	30,46
A1-ACO	33,73
A1-MTN	39,29
A1-nC5	46,18
A1-nC7	41,86
A2-NTRBC	25,22
A2-PRD	25,06
A2-CHXN	25,92
A2-TOL	27,99
A2-BENZ	27,36
A2-ACO	29,64
A2-MTN	45,98
A2-nC5	39,46
A2-nC7	35,93
R-NTRBC	29,39
R-PRD	28,51
R-CHXN	25,44
R-TOL	25,01
R-BENZ	25,01
R-ACO	25,28
R-MTN	63,51
R-nC5	29,74
R-nC7	27,83
ML-NTRBC	30,75
ML-PRD	29,74
ML-CHXN	25,94
ML-TOL	25,04
ML-BENZ	25,15
ML-ACO	25,05
ML-MTN	67,36
ML-nC5	26,90
ML-nC7	28,51

## Appendix C

Chemical sample table which is indicated the chemicals used in the research presented.


**Table C.** Chemical Compounds, CAS Registry Number, and Models.

chemical name	chemical or linear formula	CAS number	suppliers
water	H <sub>2</sub> O	7732-18-5	Onufriev et al. J. Phys. Chem. Lett. 2014, 5, 3863–3871
sodium chloride	NaCl	7647-14-5	PubChem
calcium chloride	CaCl <sub>2</sub>	10043-52-4	PubChem
heptane	C <sub>7</sub> H <sub>16</sub>	142-82-5	PubChem
toluene	C <sub>7</sub> H <sub>8</sub>	108-88-3	PubChem
nitrobenzene	C <sub>6</sub> H <sub>5</sub> NO <sub>2</sub>	98-95-3	PubChem
pyridine	C <sub>5</sub> H <sub>5</sub> N	110-86-1	PubChem
cyclohexanone	C <sub>6</sub> H <sub>10</sub> O	108-94-1	PubChem
benzene	C <sub>6</sub> H <sub>6</sub>	71-43-2	PubChem
oleic acid	C <sub>18</sub> H <sub>34</sub> O <sub>2</sub>	112-80-1	PubChem
methanol	CH <sub>3</sub> OH	67-56-1	PubChem
pentane	C <sub>5</sub> H <sub>12</sub>	109-66-0	PubChem
asphaltene A1	-	-	Acevedo et al. Energy Fuels 2010, 24, 5921–5933
asphaltene A2	-	-	Acevedo et al. Energy Fuels 2010, 24, 5921–5934
resin	-	-	Intevp. 2015-2017
maltene	-	-	Intevp. 2015-2017

**Recibido:** 27 de marzo de 2022

**Aceptado:** 15 de julio de 2022

**Silva, Carolina del Valle:** *I am Geophysical Engineer degree from the Universidad Central de Venezuela, Ph.D. in Physic from the Universidad Central de Venezuela and with a Master in Data Science from from Diplomados Online.com. I am currently a researcher at PDVSA-Intevep, Los Teques, El Tambor, Miranda state, Venezuela. My fields of interest are the theoretical-experimental studies of multiphase, multicomponent systems, disperse, non-lineal systems and meta-materials.*

 <https://orcid.org/0000-0003-4055-6428>